Received: 1 March 2019 | Revised: 16 May 2019 | Accepted: 25 June 2019

DOI: 10.1111/ejn.14506

SPECIAL ISSUE ARTICLE

EJN European Journal of Neuroscience FENS WILEY

The estrous cycle modulates rat caudate–putamen medium spiny neuron physiology

Jaime A. Willett[1,2,3,4] | **Jinyan Cao**[1,2] | **Ashlyn Johnson**[1] | **Opal H. Patel**[1] | **David M. Dorris**[1] | **John Meitzen**[1,2,5,6]

[1]Department of Biological Sciences, North Carolina State University, Raleigh, NC, USA

[2]W.M. Keck Center for Behavioral Biology, North Carolina State University, Raleigh, NC, USA

[3]Graduate Program in Physiology, North Carolina State University, Raleigh, NC, USA

[4]Grass Laboratory, Marine Biological Laboratory, Woods Hole, MA, USA

[5]Center for Human Health and the Environment, North Carolina State University, Raleigh, NC, USA

[6]Comparative Medicine Institute, North Carolina State University, Raleigh, NC, USA

Correspondence
Jaime A. Willett, Department of Biological Sciences, NC State University, Campus Box 7617, 166 David Clark Labs, Raleigh, NC 27695-7617.
Email: jawillet@ncsu.edu

Funding information
North Carolina State University; National Institute of Environmental Health Sciences, Grant/Award Number: P30ES025128; National Institute of Child Health and Human Development, Grant/Award Number: P50HD28934; National Institute of Mental Health, Grant/Award Number: R01MH109471; Grass Foundation

The peer review history for this article is available at https://publons.com/publon/10.1111/EJN.14506

Abstract

The neuroendocrine environment in which the brain operates is both dynamic and differs by sex. How differences in neuroendocrine state affect neuron properties has been significantly neglected in neuroscience research. Behavioral data across humans and rodents indicate that natural cyclical changes in steroid sex hormone production affect sensorimotor and cognitive behaviors in both normal and pathological contexts. These behaviors are critically mediated by the caudate–putamen. In the caudate–putamen, medium spiny neurons (MSNs) are the predominant and primary output neurons. MSNs express membrane-associated estrogen receptors and demonstrate estrogen sensitivity. However, how the cyclical hormone changes across the estrous cycle may modulate caudate–putamen MSN electrophysiological properties remains unknown. Here, we performed whole-cell patch-clamp recordings on male, diestrus female, proestrus female, and estrus female caudate–putamen MSNs. Action potential, passive membrane, and miniature excitatory post-synaptic current properties were assessed. Numerous MSN electrical properties robustly differed by cycle state, including resting membrane potential, rheobase, action potential threshold, maximum evoked action potential firing rate, and inward rectification. Strikingly, when considered independent of estrous cycle phase, all but one of these properties do not significantly differ from male MSNs. These data indicate that female caudate–putamen MSNs are sensitive to the estrous cycle, and more broadly, the importance of considering neuroendocrine state in studies of neuron physiology.

KEYWORDS

caudate–putamen, electrophysiology, estrous cycle, excitability, medium spiny neuron, sex differences

Abbreviations: ACSF, artificial cerebrospinal fluid; Estradiol, 17β-estradiol; KPBS, potassium phosphate buffer solution; mEPSC, miniature excitatory post-synaptic current; MSN, medium spiny neuron; s-ACSF, sucrose artificial cerebrospinal fluid; TTX, tetrodotoxin.

Edited by Thierry Charlier.

1 | INTRODUCTION

Patterns of sex steroid hormone production differ markedly between females and males over the lifespan (Gillies & McArthur, 2010). Importantly, adult female humans and

rodents, including rats, exhibit cyclical fluctuations in sex steroid hormones including 17β-estradiol (estradiol) and progesterone. In humans, these variations in hormone production occur over the ~28-day menstrual cycle. The human menstrual cycle features the follicular and luteal phases. In rodents, the timing is more rapid, occurring over the ~4- to 5-day estrous cycle (Becker et al., 2005). The rat estrous cycle phases include the diestrus, proestrus, and estrus phases. Despite the differences in length, there are similarities in the pattern of hormone fluctuation and the associated behavioral changes between humans and rodents. Most research on the adult female hormone cycle has focused on the ovary and associated reproductive functions. However, sex steroid hormones cross the blood–brain barrier to act in the central nervous system. Thus, these cyclical neuroendocrine dynamics can potentially modulate neural substrate directly to yield numerous behavioral and neural consequences. Indeed, estrous cycle effects on neuron physiology have been reported in several brain regions (Blume et al., 2017; Calizo & Flanagan-Cato, 2000; Cooke & Woolley, 2005; Hao et al., 2006; Okamoto, Hirata, Takeshita, & Bereiter, 2003; Woolley, 1998; Woolley & McEwen, 1993).

Nevertheless, most research has investigated the action of these hormone changes in the context of classical sex-specific reproductive behaviors such as lordosis (Micevych & Meisel, 2017). Numerous other behaviors that may relate to overall reproductive success are also influenced by cycle phase. For example, in both humans and rats, the mid-cycle surge in estradiol is associated with increased locomotor activity (Beatty, 1979; Becker, 2002; Becker, Snyder, Miller, Westgate, & Jenuwine, 1987; Smith, 1994), improved limb coordination (Becker et al., 1987; Hampson, 1990; Hampson & Kimura, 1988; Jennings, Janowsky, & Orwoll, 1998; Simic, Tokic, & Pericic, 2010; Zoghi, Vaseghi, Bastani, Jaberzadeh, & Galea, 2015), and, in a pathological context, decreased severity of parkinsonism (Castrioto, Hulliger, Poon, Lang, & Moro, 2010; Quinn & Marsden, 1986). All of these behaviors are mediated by the caudate–putamen, a well-conserved constituent of the basal ganglia present in both rodents and humans that is instrumental for various forms of learning, and sensorimotor performance, among other functions. Acting as a gateway region, the caudate–putamen receives numerous excitatory glutamatergic afferents, including from the cortex and the thalamus, as well as dopaminergic afferents from the substantia nigra (Kreitzer & Malenka, 2008; Palmiter, 2008). These afferents, along with internal circuitry and other inputs, ultimately converge onto the output neuron of the caudate–putamen, the GABAergic medium spiny neuron (MSN).

Medium spiny neurons comprise ≥95% of the caudate–putamen neuron population. Changes in MSN electrical activity are directly related to changes in behavior (Ferguson et al., 2011; Grillner, Hellgren, Menard, Saitoh, & Wikstrom, 2005; Tan et al., 2013). Adult female rat caudate–putamen MSNs express membrane-associated estrogen receptors α, β, and G-protein-coupled receptor 1 (GPER1; Almey, Filardo, Milner, & Brake, 2012; Almey, Milner, & Brake, 2016; Grove-Strawser, Boulware, & Mermelstein, 2010; Mermelstein, Becker, & Surmeier, 1996; Schultz et al., 2009). MSNs also famously express dopamine receptors, and there are notable differences in both the expression of these receptors and dopamine levels in the caudate–putamen over the estrous cycle in female rats and in response to exogenous estradiol in ovariectomized rats (Di Paolo, 1994; Song, Yang, Peckham, & Becker, 2019; Yoest, Quigley, & Becker, 2018). Unlike select neuron types in other brain regions, caudate–putamen MSN soma size, density, and overall caudate–putamen volume do not seem to differ by sex (Meitzen, Pflepsen, Stern, Meisel, & Mermelstein, 2011; Wong, Cao, Dorris, & Meitzen, 2016). Thus, research has largely focused on hormone-induced changes in electrophysiological properties (Meitzen, Meisel, & Mermelstein, 2018). Before puberty, female rat caudate–putamen MSNs exhibit hyperpolarized action potential threshold, decreased afterhyperpolarization magnitude, and increased slope of the evoked action potential to injected positive current curve (Dorris, Cao, Willett, Hauser, & Meitzen, 2015). However, puberty can potentially reorganize the neural substrate, including the striatal regions (Juraska, Sisk, & DonCarlos, 2013; Kopec, Smith, Ayre, Sweat, & Bilbo, 2018; Staffend, Mohr, Doncarlos, & Sisk, 2014), and introduces new sexually dimorphic hormone dynamics which can alter striatal neuron properties. Likewise, estradiol has also been shown to rapidly modulate L-type calcium channel currents and associated CREB phosphorylation in both prepubertal striatum cell culture and in adult striatum (Grove-Strawser et al., 2010; Mermelstein et al., 1996). In the early 1980s, in vivo recordings of spontaneously firing unidentified neurons in adult rats suggested that caudate–putamen excitability varies across the estrous cycle and in response to estradiol (Arnauld, Dufy, Pestre, & Vincent, 1981; Tansey, Arbuthnott, Fink, & Whale, 1983). However, for decades it has been unknown whether any cellular electrophysiological property differs by sex or across the adult female hormone cycle in an identified caudate–putamen neuron type. Based upon this literature, we suspected that MSN physiology would be sensitive to the estrous cycle. To interrogate the contributions of estrous cycle and more broadly biological sex, we thus performed whole-cell patch-clamp recordings on male, diestrus female, proestrus female, and estrus female rat caudate–putamen MSNs.

2 | MATERIALS AND METHODS

2.1 | Animals

All animal protocols were approved by Institutional Animal Care and Use Committee at North Carolina State University or

the Marine Biological Laboratory. Female ($n = 27$) and male ($n = 8$) Sprague Dawley CD IGS rats were born from timed-pregnant females purchased from Charles River. Rats were housed with their littermates and dam until weaning at age P21. After weaning, rats were housed with same sex littermates. To ensure that rats were post-puberty, age at experimental use ranged from P70 to P112. Rooms were temperature-, humidity-, and light-controlled (21–23°C; 12-hr light:12-hr darkness [34 animals]; 14-hr light: 10-hr darkness cycle [1 animal]). Rodent chow and glass bottle provided water were available ad libitum.

2.2 | Estrous cycle assessment

Estrous cycle assessment was performed using a wet mount preparation as previously described (Hubscher, Brooks, & Johnson, 2005). Briefly, females (P60 or older) were swabbed using potassium phosphate buffer solution (KPBS) ~10:00 a.m. Slides were visualized under a microscope to determine estrous cycle phase according to cell morphology as previously described (Westwood, 2008). Estrous cycle phase was confirmed via assessment of plasma concentrations of progesterone, 17β-estradiol, and testosterone in 34 of 35 animals (Table 1). At sacrifice (~10:30 a.m.), trunk blood was collected from each subject and centrifuged within 30 min. Harvested plasma was stored at −20°C until assessment at the Ligand Assay and Analysis Core at the University of Virginia using commercially available ELISA kits manufactured by Calbiotech (estradiol) or IBL (progesterone, testosterone). All protocols were validated based on the recommendations of the Endocrine Society (Wierman et al., 2014). Samples were run in duplicates. Intra- and inter-assay percent coefficient of variations was as follows: estradiol: 8.3 and 9.9, progesterone: 5.6 and 10.2, and testosterone: 5.4 and 7.8, respectively. The minimum detectable plasma estradiol, progesterone, and testosterone concentrations were 3 pg/ml, 0.15 ng/ml, and 10 ng/dl, respectively. The maximum detectable plasma concentrations were 300 pg/ml, 40 ng/ml, and 1,600 ng/dl, respectively. Plasma estradiol levels differed across estrous cycle phase in females, as expected (Butcher, Collins, & Fugo, 1974; Table 1). Overall, plasma hormone levels matched estrous cycle phase identification from vaginal cytology assessment, confirming the validity of this method for estrous cycle phase identification.

2.3 | Electrophysiology

2.3.1 | Acute brain slice preparation

Methods for preparing brain slices for electrophysiological recordings were as previously described (Dorris, Hauser, Minnehan, & Meitzen, 2014). Rats were deeply anesthetized with isoflurane gas and killed by decapitation. Trunk blood was collected at sacrifice for serum hormone levels assessment. The brain was dissected rapidly into ice-cold, oxygenated sucrose artificial CSF (s-ACSF) containing (in mM) 75 sucrose, 1.25 NaH_2PO_4, 3 $MgCl_2$, 0.5 $CaCl_2$, 2.4 Na pyruvate, 1.3 ascorbic acid from Sigma-Aldrich, and 75 NaCl, 25 $NaHCO_3$, 15 dextrose, 2 KCl from Fisher; osmolarity 295–305 mOsm, pH 7.2–7.4. Serial 300 μm coronal brain slices containing the caudate–putamen were prepared using a vibratome and incubated in regular ACSF containing (in mM) 126 NaCl, 26 $NaHCO_3$, 10 dextrose, 3 KCl, 1.25 NaH_2PO_4, 1 $MgCl_2$, 2 $CaCl_2$, 295–305 mOsm, pH 7.2–7.4 for 30 min at 35°C and at least 30 min at room temperature (21–23°C). Slices were stored, submerged in room temperature, and oxygenated ACSF for up to 5 hr after sectioning in a large volume bath holder.

2.3.2 | Electrophysiological recording

After resting for ≥1 hr after sectioning, slices were placed in a Zeiss Axioscope equipped with IR-DIC optics, a Dage IR-1000 video camera, and 10× and 40× lenses with optical zoom. Slices were superfused with oxygenated ACSF heated to 27 ± 1°C (Male: 27 ± 1°C; Female: 27 ± 1°C, $p > .05$). Whole-cell patch-clamp recordings were made from MSNs in the caudate–putamen (Figure 1). Recordings were made using glass electrodes (5–12 MΩ) containing (in mM) 115 K D-gluconate, 8 NaCl, 2 EGTA, 2 $MgCl_2$, 2 MgATP, 0.3 NaGTP, 10 phosphocreatine from Sigma-Aldrich and 10 HEPES from Fisher, 285 mOsm, pH 7.2–7.4. Signals were amplified, filtered (2 kHz), and digitized (10 kHz) with a MultiClamp 700B amplifier attached to a Digidata 1550

TABLE 1 Plasma sex steroid hormone concentrations in adult rats

Hormone	Diestrus	Proestrus	Estrus	Males	Statistics (F/KW, p)
17β-estradiol (pg/ml)	3.59 ± 0.42 (10)[a,*]	10.01 ± 1.37 (8)[b]	3.10 ± 0.07 (8)[a,*]	–	16.94, .0002
Progesterone (ng/ml)	37.34 ± 1.16 (10)[a]	22.19 ± 4.79 (8)[b]	28.29 ± 4.69 (8)[a,b]	–	4.58, .0212
Testosterone (ng/ml)	–	–	–	5.83 ± 1.71 (8)	–

Note: Values are mean ± *SEM*. Numbers in parentheses indicate animal sample size. Superscript letters indicate statistically significant differences across groups. The presence of an asterisk (*) denotes a non-normal distribution.

Abbreviation: –, Not measured.

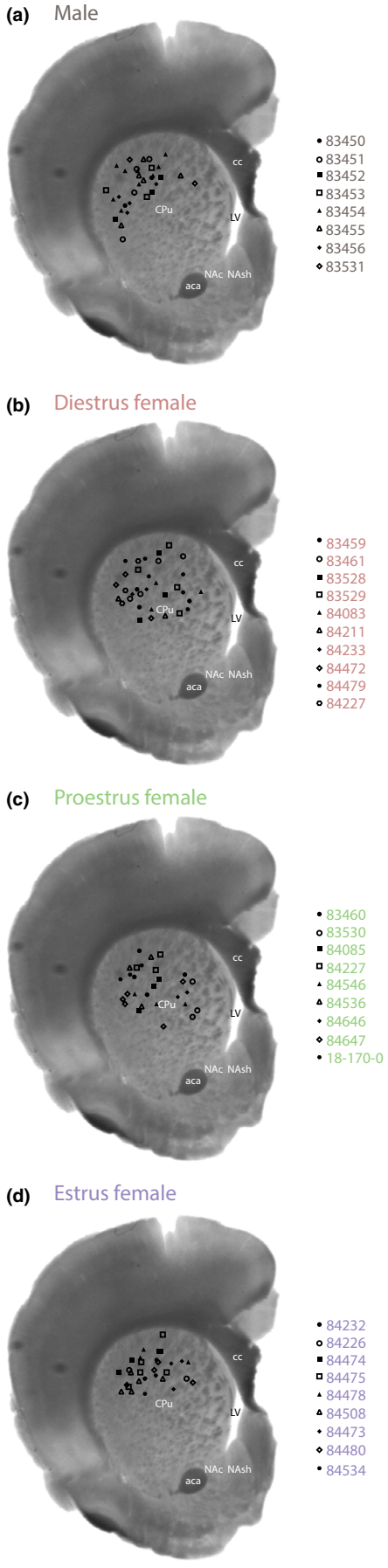

system and a personal computer using pClamp 10 software. Membrane potentials were corrected for a calculated liquid junction potential of −13.5 mV (Dorris et al., 2015). Using previously described procedures, recordings were made in current clamp to assess neuronal electrophysiological properties. MSNs were identified by their medium-sized somas, the presence of a slow ramping subthreshold depolarization in response to low-magnitude positive current injections, a hyperpolarized resting potential more negative than −65 mV, inward rectification, and prominent spike afterhyperpolarization (Belleau & Warren, 2000; O'Donnell & Grace, 1993).

In a subset of recordings, oxygenated ACSF containing the $GABA_A$ receptor antagonist picrotoxin (150 μM; Fisher) and the voltage-gated sodium channel blocker tetrodotoxin (TTX, 1 μm, Abcam Biochemicals) was applied to the bath to abolish action potentials and inhibitory post-synaptic current events. Once depolarizing current injection no longer elicited an action potential, MSNs were voltage-clamped at −70 mV and miniature excitatory post-synaptic current events (mEPSCs) were recorded for 5 min. This preparation detects AMPA-mediated mEPSCs and has been confirmed by our laboratory (Proano, Morris, Kunz, Dorris, & Meitzen, 2018). Input and series resistance was monitored for changes, and cells were discarded if resistance changed more than 20% or featured action potential amplitudes of less than 35 mV.

2.3.3 | Data analysis

Basic electrophysiological properties and action potential characteristics were analyzed using pClamp 10. After break-in, the resting membrane potential was first allowed to stabilize ~1–2 min, as in Mu et al. (2010). At least three series of depolarizing and hyperpolarizing current injections were applied to elicit basic neurophysiological properties (Dorris et al., 2015). Most properties measured followed the definitions of Willett et al. (2018), which were originally derived from those of Perkel and colleagues (Farries, Meitzen, & Perkel, 2005; Farries & Perkel, 2000, 2002; Meitzen, Weaver, Brenowitz, & Perkel, 2009). For each neuron, measurements were made of at least three action potentials generated from minimal current injections. These measurements were then averaged to generate the reported action potential measurement for that neuron. For action potential measurements, only

FIGURE 1 Schematic of whole-cell patch-clamped medium spiny neuron (MSN) locations in male and female rat caudate–putamen. (a) Male. (b) Diestrus female. (c) Proestrus female. (d) Estrus female. MSNs recorded from different animals are indicated by different symbols; animal identification number is at right. AC, anterior commissure; CC, corpus callosum; CPu, caudate–putamen; LV, lateral ventricle; NaC, nucleus accumbens core; NaSH, nucleus accumbens shell

the first generated action potential was used. Action potential threshold was defined as the first point of sustained positive acceleration of voltage ($\delta^2V/\delta t^2$) that was also more than three times the SD of membrane noise before the detected threshold (Baufreton, Atherton, Surmeier, & Bevan, 2005). Rectified range input resistance, inward rectification, and percent inward rectification were calculated as described previously (Belleau & Warren, 2000). The slope of the linear range of the evoked firing rate to positive current curve (FI slope) was calculated from the first current stimulus which evoked an action potential to the first current stimulus that generated an evoked firing rate that persisted for at least two consecutive current stimuli. Input resistance in the linear, non-rectified range was calculated from the steady-state membrane potential in response to −0.02 nA hyperpolarizing pulses. The membrane time constant was calculated by fitting a single exponential curve to the membrane potential change in response to −0.02 nA hyperpolarizing pulses. Membrane capacitance was calculated using the following equation: capacitance = time constant of the membrane/input resistance. mEPSC frequency, amplitude, and decay were analyzed off-line using Mini Analysis (Synaptosoft, http://www.synaptosoft.com/MiniAnalysis/). Threshold was set at a minimum value of 5 pA, and accurate event detection was validated by visual inspection.

2.3.4 | Statistics

Given that this experiment does not feature a balanced design (i.e., the males do not exhibit an estrous cycle), we employed a hypothesis-driven statistical analysis, similar to previous studies with comparable analysis challenges (Cao et al., 2015; Hicks et al., 2016). First, to probe for baseline sex differences, two-tailed *t* tests or Mann–Whitney *U* tests were employed to compare male and female values independent of estrous cycle phase (Prism version 6.0; GraphPad Software). Independent of the outcome of this first analysis, female data were then disaggregated by estrous cycle phase and compared using one-way ANOVAs or Kruskal–Wallis tests. Linear regressions were then used to further analyze select datasets. Post hoc tests employed were Newman–Keuls or Dunn's multiple comparison tests as appropriate. Distributions were analyzed for normality with the D'Agostino and Pearson omnibus normality test. For two-tailed t tests and Mann–Whitney *U* tests, actual differences between means and medians along with 95% confidence intervals are reported to indicate magnitude and directions of changes. p values $< .05$ were considered a priori as significant. Data are presented as mean ± *SEM*.

3 | RESULTS

We recorded 122 MSNs in the caudate–putamen of adult rat male and females. To meet our primary goal of understanding the contributions of biological sex and the female estrous cycle toward modulating caudate–putamen MSN function, we first conducted analyses by sex to detect any overall sex differences present and then further analyses by estrous cycle phase within the female MSN dataset to compare between female MSNs in diestrus, proestrus, and estrus. Aggregate electrophysiological properties of all recorded MSNs and relevant statistics are presented in Tables 2 and 3.

3.1 | Action potential and resting membrane potential properties differ by sex or by estrous cycle phase

Individual action potentials were elicited using positive current injections (Figure 2a). We found an overall sex difference in the afterhyperpolarization peak, with male MSNs exhibiting larger afterhyperpolarization peaks than female MSNs (Figure 2b). This finding is consistent with previous recordings in prepubertal rat caudate–putamen MSNs, which likewise observed a larger afterhyperpolarization peak in male compared with female MSNs (Dorris et al., 2015). Afterhyperpolarization peak did not differ across estrous cycle state (Figure 2b). While no other individual action potential property exhibited an overall sex difference (Table 2), further analysis of the female MSNs by estrous cycle stage revealed cycle-dependent changes across the entire spectrum of MSN electrophysiological properties.

Regarding resting membrane potential, female MSNs in proestrus demonstrated a hyperpolarized resting membrane potential compared with female MSNs in diestrus (Figure 2c). The rheobase, or the amount of current necessary to elicit an action potential from the MSN, was dramatically elevated for female MSNs in estrus compared with female MSNs in both diestrus and proestrus (Figure 2d). Female MSNs in proestrus demonstrated a significantly hyperpolarized action potential threshold compared with female MSNs in both diestrus and estrus (Figure 2e). Consistent with this change in threshold, the action potential amplitude was significantly larger in female MSNs in proestrus compared with female MSNs in both diestrus and estrus (Figure 2f). This change in amplitude is dependent upon changes in threshold. Supporting this interpretation, action potential threshold demonstrates a significant negative correlation with action potential amplitude (Figure 2g). This indicates that neurons with hyperpolarized thresholds exhibit action potentials with increased amplitudes. Another canonical feature of MSNs is a pronounced delay to the first action potential, reflecting the presence of the slowly inactivating A-type K current, responsible for the slow ramping subthreshold depolarization (Nisenbaum, Xu, & Wilson, 1994). No sex or estrous cycle phase differences were observed in this property (Figure 2h). Likewise, no sex or estrous cycle stage differences were detected in action

TABLE 2 Electrophysiological properties of medium spiny neurons in adult rat caudate–putamen

Property	Male	Female	Statistics D, t/U, *p*	Diestrus	Proestrus	Estrus	Statistics *F*/KW, *p*
Resting membrane potential (mV)	−89.56 ± 0.58, (30)*	−88.86 ± 0.33, (89)*	1.072 [−0.1080, 1.754], 1,051, .0825	−88.28 ± 0.43 (31)*	−89.89 ± 0.64 (28)	−88.50 ± 0.63 (30)*	6.527, .0342
Delay to first action potential (ms)	432.34 ± 14.46, (26)	414.21 ± 8.28, (83)*	6.125 [−47.27, 20.65], 959, .3978	417.67 ± 14.00 (30)	414.03 ± 15.95 (24)	410.77 ± 13.81 (29)*	0.094, .9217
Rheobase (nA)	0.26 ± 0.019, (31)	0.27 ± 0.01, (91)	0.009416 [−0.03501, 0.05385], 0.42, .6755	0.25 ± 0.01 (33)^{a,b,c}	0.25 ± 0.02 (28)^{b}	0.32 ± 0.02 (30)^{c}	3.70, .0287
AP threshold (mV)	−52.77 ± 1.15, (31)*	−52.37 ± 0.81, (91)*	0.8300 [−2.562, 2.980], 1,382, .8690	−51.28 ± 1.26 (33)*^{,a}	−57.22 ± 1.20 (28)^{b}	−49.04 ± 1.35 (30)^{a}	18.45, .0007
AP width at half-peak amplitude (ms)	1.85 ± 0.07, (31)	1.81 ± 0.03, (91)	−0.03976 [−0.1741, 0.09462], 0.5858, .5591	1.83 ± 0.04 (33)	1.74 ± 0.08 (28)	1.86 ± 0.04 (30)	1.19, .6153
AP amplitude (mV)	68.67 ± 2.27, (31)	66.65 ± 1.27, (91)	−2.023 [−7.076, 3.031], 0.79, .4297	65.01 ± 1.88 (33)^{a,b}	73.34 ± 2.57 (28)^{a}	62.20 ± 1.72 (30)^{b}	7.506, .0072
AHP peak amplitude (mV)	−10.36 ± 0.46, (31)*	−9.10 ± 0.23, (91)*	1.428 [0.3548, 2.036], 955.5, .0070	−9.40 ± 0.33 (33)	−8.72 ± 0.35 (28)	−9.11 ± 0.50 (30)*	1.941, .3800
AHP time to peak (ms)	28.89 ± 1.13, (31)	28.00 ± 0.73, (90)*	−1.353 [−3.937, 1.683], 1,249, .3871	28.84 ± 0.96 (32)	27.12 ± 1.27 (28)	27.92 ± 1.52 (30)*	1.54, .6841
FI slope (Hz/nA)	137.32 ± 7.69, (31)	151.49 ± 5.27, (91)*	12.91 [−6.688, 30.04], 1,197, .2110	148.27 ± 7.32 (33)*	170.29 ± 12.01 (28)	137.49 ± 7.24 (30)	3.918, .2211
Time constant of the membrane (ms)	10.24 ± 1.33, (30)*	8.53 ± 0.48, (89)*	−1.300 [−2.506, 0.5146], 1,137, .2277	8.51 ± 0.65 (33)*	10.20 ± 1.22 (27)*	6.98 ± 0.50 (29)	5.412, .0668
Linear range input resistance (MΩ)	89.44 ± 8.43, (30)*	84.82 ± 3.45, (89)*	3.461 [−12.53, 14.45], 1,318, .9200	87.83 ± 4.94 (32)*	81.41 ± 7.67 (28)*	84.80 ± 5.43 (29)	1.319, .5170
Capacitance (pF)	130.05 ± 15.68, (30)*	109.41 ± 6.12, (89)*	−12.24 [−32.22, 9.978], 1,168, .3094	101.84 ± 9.06 (33)*	136.33 ± 12.80 (27)	92.95 ± 8.72 (29)	7.744, .0208
Rectified range input resistance (MΩ)	78.79 ± 6.59, (30)*	78.38 ± 3.30, (89)*	3.141 [−10.48, 14.35], 1,298, .8242	80.76 ± 4.70 (32)	71.25 ± 6.39 (28)	82.63 ± 6.13 (29)	1.098, .3381
Percent inward rectification (%)	89.47 ± 1.12, (30)*	92.34 ± 0.93, (89)	1.712 [−0.6577, 5.311], 1,073, .1098	91.92 ± 1.18 (32)^{a,b,c,d}	88.83 ± 1.76 (28)^{a,c,d}	96.18 ± 1.67 (29)^{b,d}	7.111, .0286
Inward rectification (MΩ)	8.48 ± 1.35, (29)*	6.38 ± 0.95, (89)*	−1.542 [−4.476, 0.6471], 1,068, .1029	7.07 ± 1.04 (32)*^{,a,b,c,d}	9.95 ± 2.13 (28)^{a,c,d}	2.17 ± 1.46 (29)*^{,b,d}	6.943, .0311
Minimum firing rate (Hz)	2.32 ± 0.34, (31)*	2.63 ± 0.18, (91)*	1 [0.0, 1.000], 1,179, .1596	2.43 ± 0.31 (30)*	2.63 ± 0.33 (30)*	2.81 ± 0.31 (31)*	1.022, .5165
Maximum firing rate (Hz)	33.23 ± 1.72, (31)	39.14 ± 0.89, (91)	5.917 [2.314, 9.520], 3.252, .0015	38.60 ± 1.58 (30)^{a,b}	36.70 ± 1.55 (30)^{a,c}	42.03 ± 1.35 (31)^{b}	3.286, .0420

Notes: Values are mean ± *SEM*. Numbers in parentheses indicate number of neurons recorded. Shaded values indicate statistical significance. D = difference between medians or means followed by the 95% confidence intervals. Superscript letters indicate statistically significant differences across groups. The presence of an asterisk (*) denotes a non-normal distribution.

Abbreviations: AHP, afterhyperpolarization; AP, action potential; FI, frequency of evoked action potentials to injected depolarizing current.

TABLE 3 mEPSC properties recorded from medium spiny neurons in adult rat caudate–putamen

Property	Male	Female	Statistics D, U, *p*	Diestrus	Proestrus	Estrus	Statistics *F*/KW, *p*
Frequency (Hz)	2.18 ± 0.35 (15)*	2.71 ± 0.24, (38)*	0.5129 [−0.07374, 1.183], 196, .0798	2.89 ± 0.39 (19)*	2.84 ± 0.66 (6)	2.39 ± 0.28 (13)	0.03, .9872
Amplitude (pA)	12.39 ± 0.77 (15)	11.70 ± 0.41, (38)*	−0.2849 [−1.930, 1.021], 245, .4371	11.47 ± 0.61 (19)*	13.42 ± 1.37 (6)	11.25 ± 0.49 (13)	2.20, .3328
Decay (ms)	3.15 ± 0.19 (15)	3.47 ± 0.10, (38)*	0.3200 [−0.06208, 0.7635], 194, .0731	3.52 ± 0.13 (19)*	2.80 ± 0.37 (6)	3.69 ± 0.10 (13)	4.67, .0967

Note: Values are mean ± *SEM*. Numbers in parentheses indicate number of neurons recorded. The presence of an asterisk (*) denotes a non-normal distribution. D = difference between medians or means followed by the 95% confidence intervals. Superscript letters indicate statistically significant differences across groups.

potential width at half-peak (Table 2). Collectively, these data indicate MSN action potential properties are sensitive to the estrous cycle. Furthermore, when sex is analyzed independent of estrous cycle, the majority of these differences in action potential properties remain undetected.

3.2 | Medium spiny neuron excitability differs by sex in an estrous cycle-dependent manner

Given that there were differences in rheobase and other action potential properties detected between cycle phases within females, this suggests that there may be differences in the overall excitability of MSNs at least as indicated by evoked firing rate properties (Figure 3a). To assess this possibility, we plotted the frequency of action potentials evoked by depolarizing current injection curves for individual caudate–putamen MSNs to compare the contributions of biological sex (Figure 3b) and estrous cycle phase (Figure 3c). Note that Figure 3b,c depicts evoked action potential rate versus injected current curves up to each MSN's maximum evoked action potential firing rate. After that point, MSN firing rate either remained constant or decreased. The maximum evoked firing rate was significantly increased in female caudate–putamen MSNs compared with male MSNs (Figure 3d). This sex difference is estrous cycle phase-dependent. Female caudate–putamen MSNs in estrus exhibit higher maximum evoked firing rates than female caudate–putamen MSNs in proestrus. To further explore the role of the estrous cycle in modulating maximum evoked firing rate and rheobase, we then analyzed whether these excitability metrics correlated with one another in female MSNs (Figure 3e). Across female MSNs regardless of estrous cycle phase, maximum firing rate and rheobase positively correlated with each other (Figure 3e, $F = 10.28$, $R^2 = .11$, $p = .0019$). This association was driven by MSNs recorded during proestrus ($F = 11.70$, $R^2 = .34$, $p = .0023$), but not diestrus ($p = .8259$) or estrus ($p = .0786$). This indicates that these properties are concomitant during select estrous cycle phases such as proestrus. To assess a different aspect of cellular excitability, for individual MSNs we also calculated the slope of the evoked firing rate to positive current curve (FI Slope, Figure 3f). In a previous study (Dorris et al., 2015), this was a property that was significantly increased in female compared with male prepubertal caudate–putamen rat MSNs. In adult MSNs, no sex difference in FI Slope was statistically detected, nor was this property significantly modulated across the estrous cycle in females, although a non-significant increase in females compared with males and during female proestrus is noted (Figure 3f). Similarly, no sex or estrous cycle differences were detected in minimum evoked firing rates (Table 2). Overall, these data indicate that excitability is robustly increased in females compared with males, with estrous cycle phase prominently modulating female MSN maximum evoked action potential firing rate.

3.3 | Caudate–putamen medium spiny neuron input resistance and inward rectification differ across the estrous cycle in females

In response to hyperpolarizing current pulses, MSNs typically exhibit input resistance that varies strongly with membrane potential and marked time-independent inward rectification that is especially noticeable at highly negative membrane potentials (Kawaguchi, Wilson, & Emson, 1989). We assessed these properties in males and females in different phases of the estrous cycle by injecting a series of increasingly hyperpolarizing current pulses (Figure 4a). One female MSN in diestrus exhibited values over 10 standard deviations from the mean and was excluded as an outlier in analyses associated with Figure 5b–f. Considered independent of estrous cycle phase, we detected no differences between males and females in the input resistance in both the linear and rectified ranges (Figure 4b). However, when considered in the context of estrous cycle, prominent differences seemed to emerge in the rectified but not linear ranges (Figure 4c). To further explore this possibility, we tested whether the measured input resistance differed between the

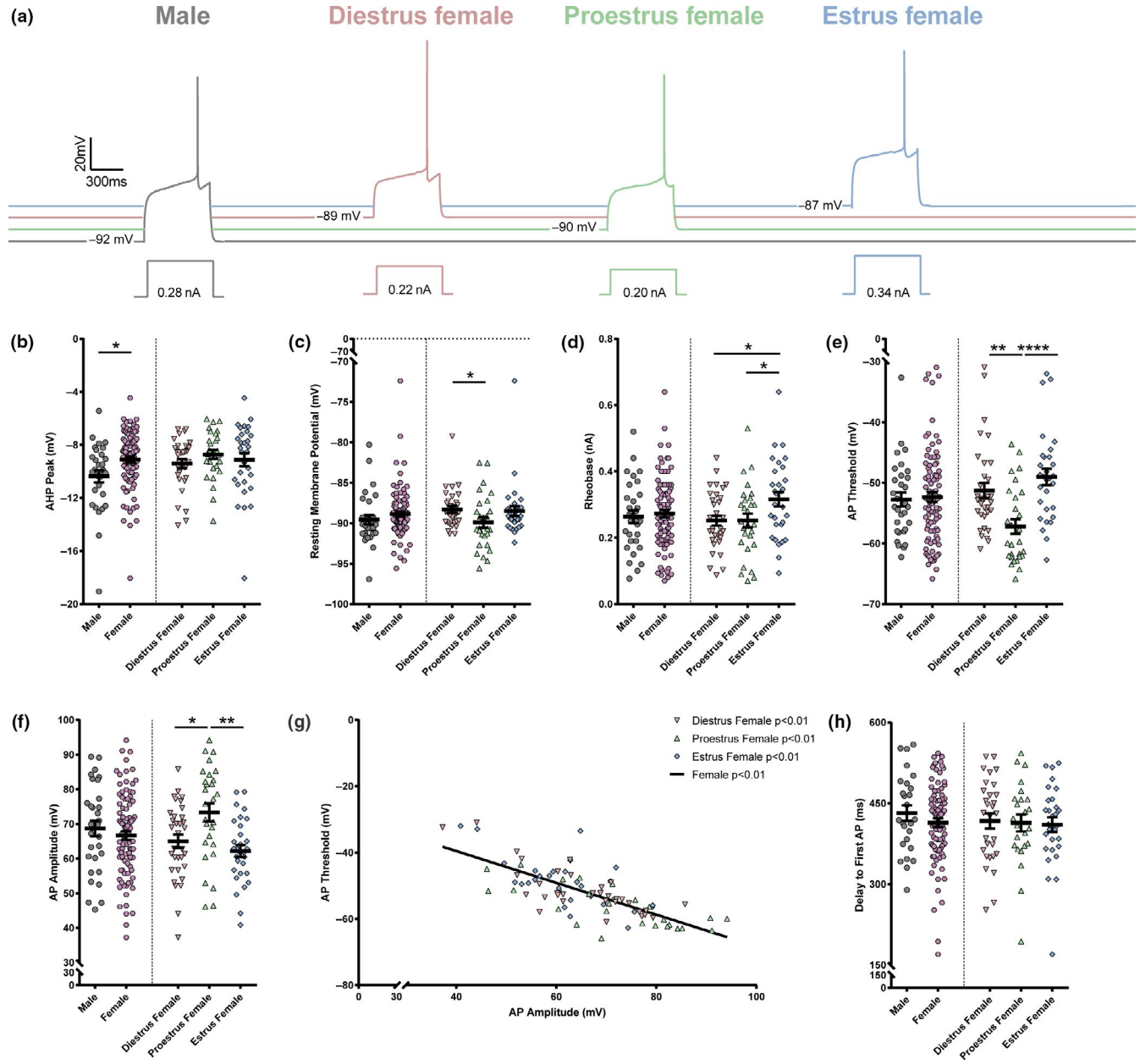

FIGURE 2 Action potential properties differ by sex or by estrous cycle stage. (a) Voltage response of a male, diestrus female, proestrus female, and estrus female MSN to a single depolarizing current injection at rheobase. Threshold measurements are indicated with arrows. Resting membrane potential measurements are listed to the left of each trace. (b) The action potential afterhyperpolarization peak is smaller in female MSNs relative to male MSNs and does not differ across estrous cycle phase. (c) Resting membrane potential differs by estrous cycle phase and is hyperpolarized in proestrus female MSNs compared with diestrus female MSNs. (d) Action potential rheobase differs by estrous cycle phase and is elevated in estrus female MSNs compared with diestrus and proestrus female MSNs. (e) Action potential threshold differs by estrous cycle phase and is hyperpolarized in proestrus female MSNs compared with diestrus and estrus female MSNs. (f) Action potential amplitude differs by estrous cycle phase and is elevated in proestrus female MSNs relative to diestrus and estrus female MSNs. (g) The estrous cycle-dependent change in action potential threshold negatively correlates with the estrous cycle-dependent change in action potential amplitude. These properties are significantly negatively correlated when female MSNs are analyzed independent of estrous cycle phase, as well as when diestrus, proestrus, and estrus cycle phases are assessed separately. (h) The delay to the first action potential does not differ by sex or by estrous cycle stage. AHP, afterhyperpolarization; AP, action potential; *$p < .05$; **$p < .01$; ****$p < .0001$

linear and rectified ranges as expected from previous work in MSNs of unspecified sex. This expected decrease in input resistance was present in all groups except for female caudate–putamen MSNs in estrus (Figure 4d; $p < .0001$ for diestrus and proestrus phases; $p = .1498$ for estrus), which demonstrated little to no decrease. To confirm the apparent diminution of inward rectification in estrus, we assessed the total magnitude of inward rectification (Figure 4e). No sex

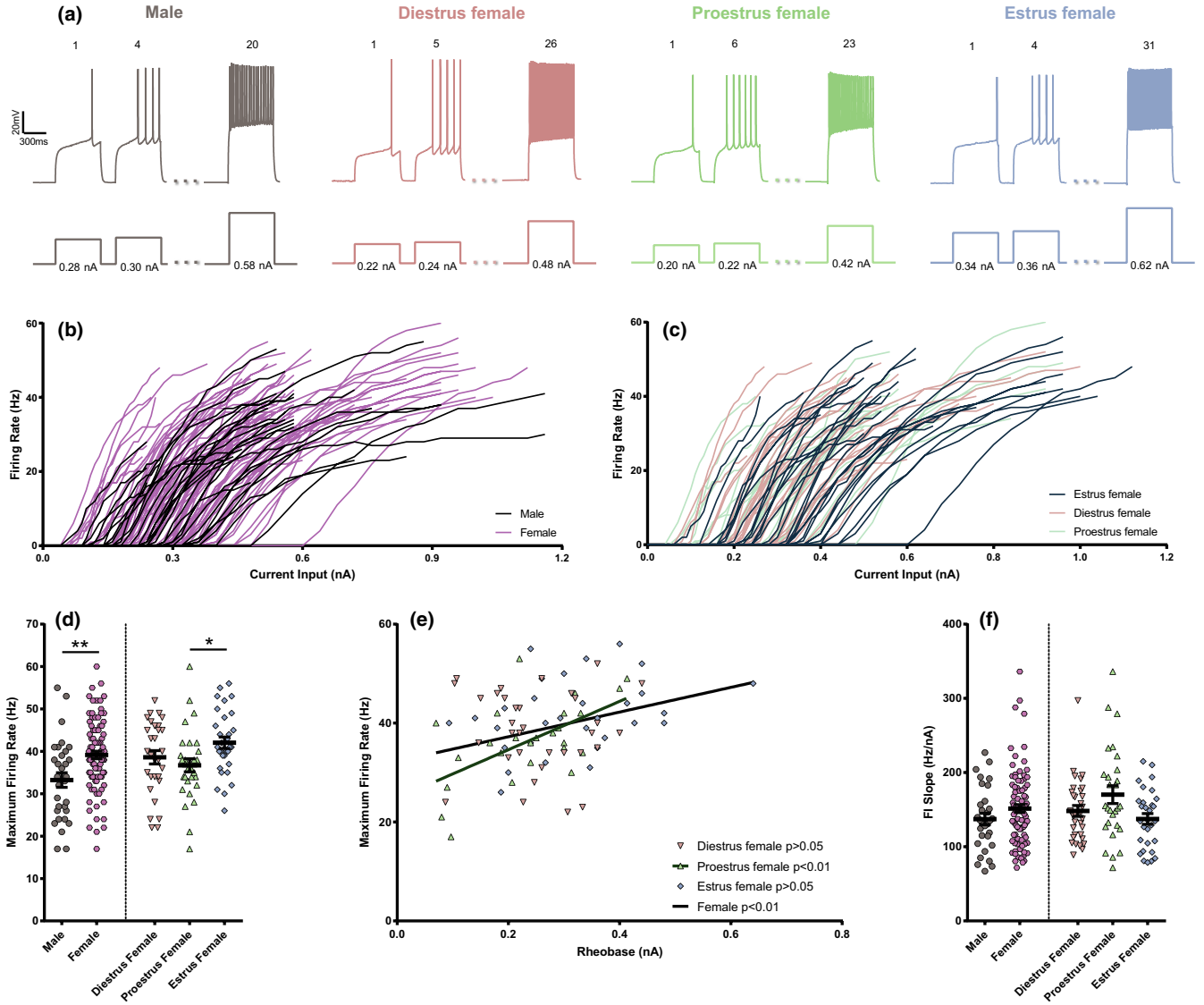

FIGURE 3 Action potential firing rates evoked by depolarizing current injections vary by estrous cycle phase. (a) Action potential firing rates evoked by depolarizing current injections from MSNs recorded in a male, diestrus female, proestrus female, and estrus female. The number of action potentials elicited for each stimulation is listed above each trace. (b) Action potential firing rates evoked by depolarizing current injections of individual MSNs differs by sex. (c) Action potential firing rates evoked by depolarizing current injections of individual female MSNs differs by estrous cycle phase. (d) The maximum action potential firing rate evoked by positive current stimulation differs by sex and estrous cycle phase. Maximum firing rate is greater for female MSNs compared with male MSNs and is elevated in estrus female MSNs relative to proestrus females. (e) Across female MSNs regardless of estrous cycle phase, maximum firing rate and rheobase positively correlated with each other. These properties likewise correlate during the proestrus phase, but not in the diestrus or estrus phases. (f) The slopes of the evoked firing rate to positive current curve (FI Slope) in individual MSNs do not differ by sex or by estrous cycle stage. FI slope, slope of the evoked action potential to depolarizing current injection curve; $*p < .05$; $**p < .01$

difference was detected in this measure. However, a significant effect of estrous cycle phase was detected with female MSNs in estrus showing the least amount of inward rectification. To determine whether this difference was mediated by a difference in the rectified range input resistance within each MSN, we normalized the data by calculating the percent inward rectification (percent inward rectification = rectified range input resistance/linear range input resistance × 100). Using this metric, a percent inward rectification value of 100% indicates that no inward rectification is present. As predicted by the previous measures, we detected a significant difference between female caudate–putamen MSNs in proestrus and estrus with MSNs in estrus displaying significantly less rectification (Figure 4f).

To complete our analysis of the passive properties of the membrane, we calculated the time constant of the membrane and the capacitance. While we detected no significant effect of sex or estrous cycle phase on the time constant of

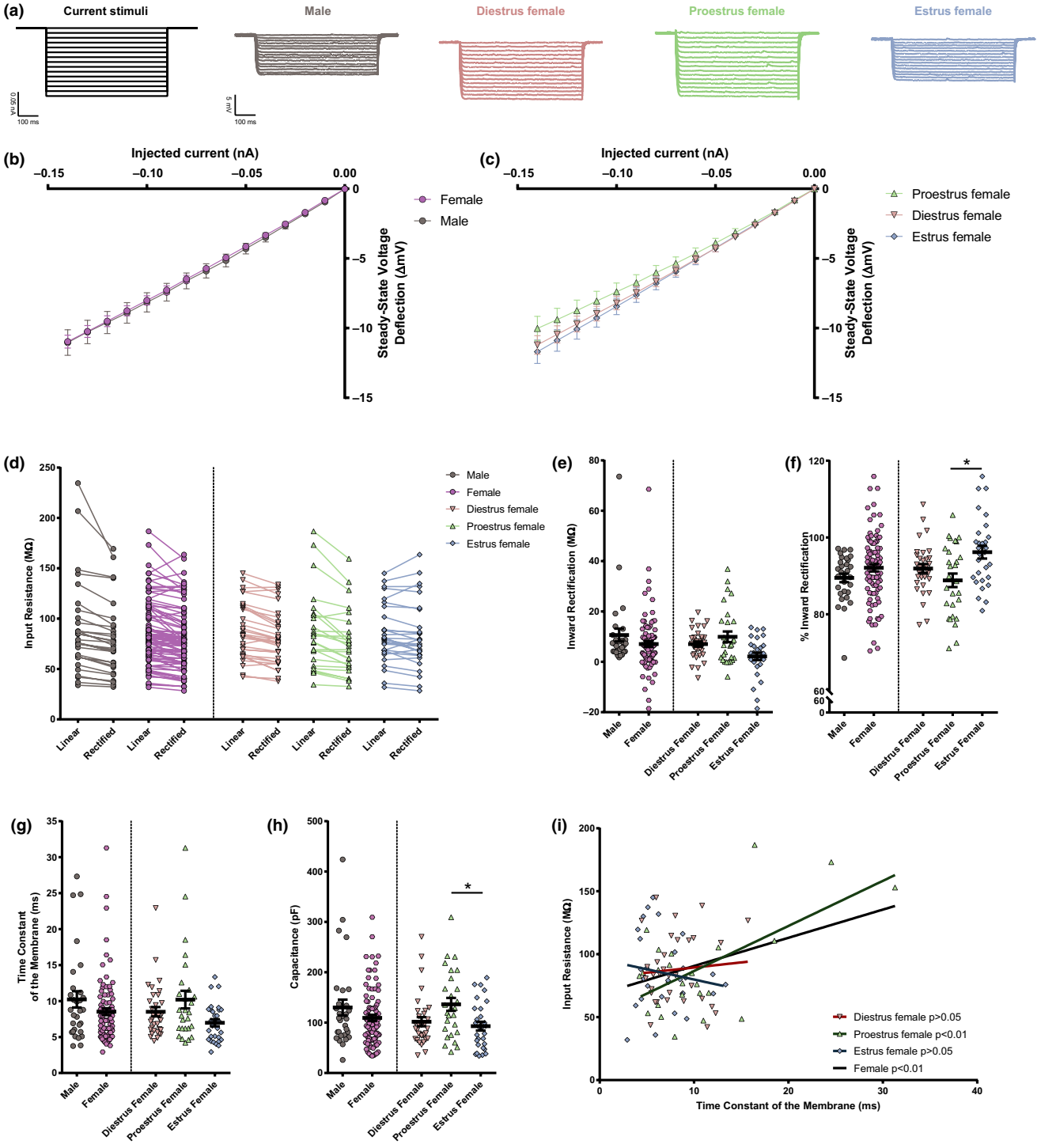

FIGURE 4 Inward rectification and capacitance vary by estrous cycle phase. (a) Voltage responses of a male, diestrus female, proestrus female, and estrus female MSNs to a series of hyperpolarizing current injections. (b) The injected current to steady stage voltage deflection curve (IV curve) does not differ by sex when estrous phase is not considered. (c) The injected current to steady stage voltage deflection curve (IV curve) differs by estrous cycle phase. (d) The expected decrease in input resistance from the linear to the rectified range differs by estrous cycle phase. The magnitude of the decrease in input resistance was small or nonexistent in estrous female MSNs. (e) The total magnitude of inward rectification differs by estrous cycle phase and is decreased in estrus female MSNs relative to other phases. (f) The percent inward rectification differs by estrous cycle phase and is decreased in estrus female MSNs relative to other phases. We note that for this metric, increased inward rectification is indicated by a decreased percent inward rectification. (g) The time constant of the membrane trended toward differing by estrous cycle phase, with decreased values during the estrus phase compared with other phases. (h) The membrane capacitance differs by estrous cycle phase and is elevated in proestrus female MSNs compared with estrus females. (i) Linear range input resistance and the time constant of the membrane positively correlate when female MSNs are analyzed independent of estrous cycle phase, as well as during the diestrus and proestrus phases. These values do not correlate during the estrus phase. *$p < .05$; **$p < .01$

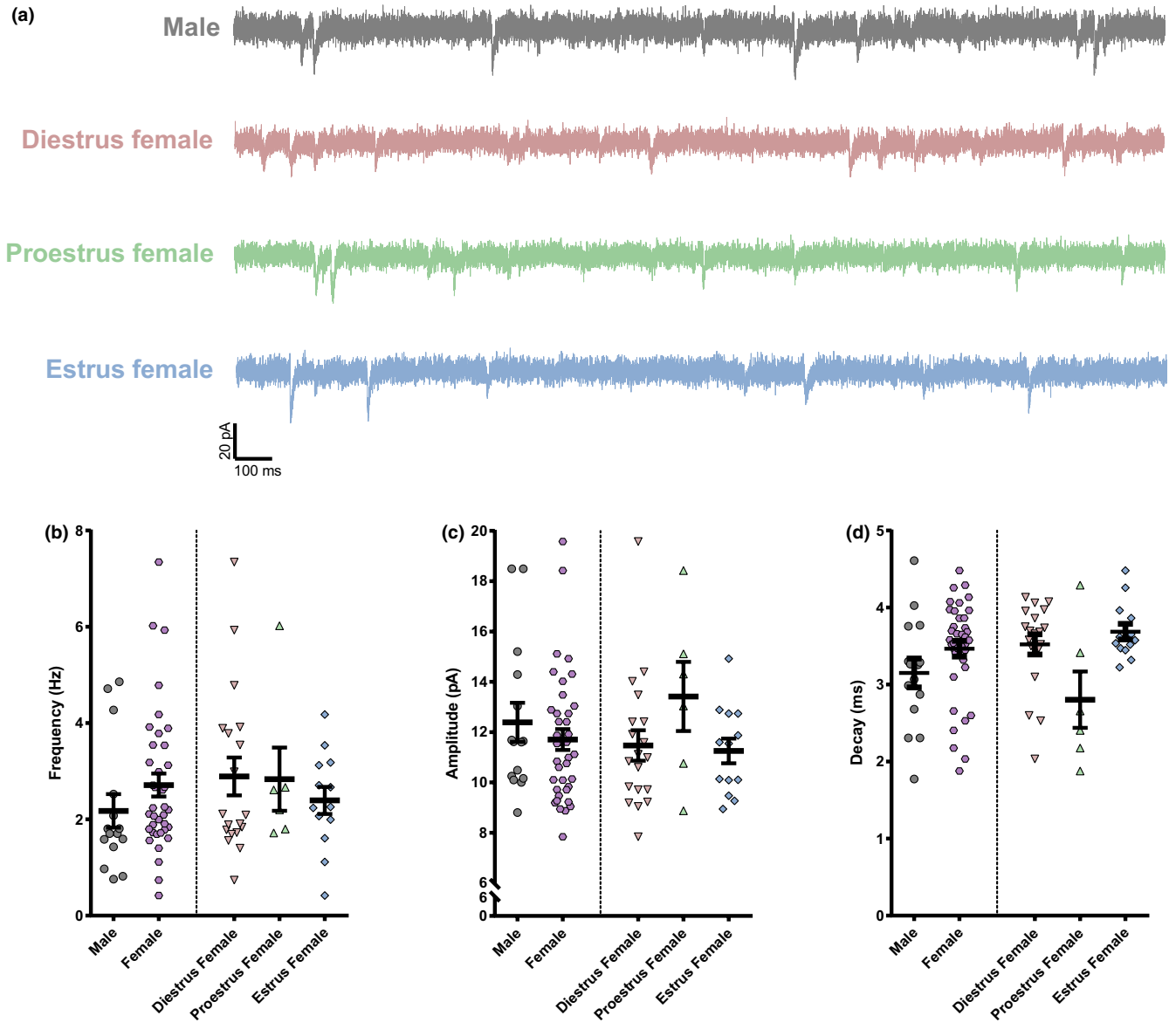

FIGURE 5 Excitatory synaptic properties as assessed by miniature excitatory synaptic current (mEPSC) analysis do not differ by sex or estrous cycle state. (a) Representative examples of miniature excitatory post-synaptic currents (mEPSCs) from male, diestrus female, proestrus female, and estrus female MSNs. The following mEPSC properties do not differ by sex or estrous cycle phase: (b) mEPSC frequency. (c) mEPSC amplitude. (d) mEPSC decay

the membrane, there was a trend toward significance regarding estrous cycle phase with values in MSNs in estrus being decreased relative to MSNs in proestrus (Figure 4g). A significant difference in the membrane capacitance between female caudate–putamen MSNs in estrus and female MSNs in proestrus was detected (Figure 4h). This change in capacitance during proestrus was driven by changes in the time constant of the membrane as significant correlations were detected between the time constant of the membrane and the input resistance for this phase (Figure 4i; Diestrus: $F = 0.19$, $R^2 = .01$, $p = .6636$; Proestrus: $F = 12.91$, $R^2 = .37$, $p = .0016$; Estrus: $F = 0.61$, $R^2 = .02$, $p = .4404$; Overall: $F = 8.96$, $R^2 = .10$, $p = .0036$). Collectively, these data indicate that fundamental changes in passive membrane dynamics of the neuron occur over the course of the estrous cycle in female caudate–putamen MSNs.

3.4 | Excitatory synaptic properties do not differ by sex or estrous cycle phase

The previous work in prepubertal caudate–putamen and nucleus accumbens shell MSNs detected no sex differences in mEPSC properties (Dorris et al., 2015; Willett et al., 2016). However, research has indicated that MSNs in the striatal region nucleus accumbens core exhibit differences in mEPSC frequency and amplitude across the estrous cycle in adult

female rats (Proano et al., 2018) and that sex-specific excitatory synapse anatomy is also present (Bayless & Daniel, 2015; Forlano & Woolley, 2010; Wissman, May, & Woolley, 2012; Wissman, McCollum, Huang, Nikrodhanond, & Woolley, 2011). Thus, it is possible that mEPSC properties may likewise differ across the estrous cycle in adult caudate–putamen. To test this hypothesis, we voltage-clamped adult caudate–putamen MSNs to −70 mV and recorded mEPSCs in the presence of TTX and PTX (Figure 5a). Similar to prepubertal caudate–putamen, we detected no effect of biological sex or estrous cycle phase in the frequency (Figure 5b), amplitude (Figure 5c), or decay (Figure 5d) of mEPSCs recorded from adult caudate–putamen MSNs. This suggests that the differences observed in overall excitability are not occurring with concomitant changes in excitatory synapse properties.

4 | DISCUSSION

This study illustrates how adult female caudate–putamen MSN electrophysiological properties differ across the estrous cycle, leading to cycle-dependent sex differences in properties that are otherwise masked or oversimplified when only analyzed by sex. To assess MSN excitability over the estrous cycle, we analyzed a comprehensive battery of electrophysiological properties. Aspects of MSN excitability differed across the estrous cycle, but in a complex and phase-specific manner (Figure 6). We further found that these cyclical changes are specific to intrinsic excitability and do not extend to changes in excitatory synapse properties. Across all cycle phases, the relationship between caudate–putamen MSN resting membrane potential, action potential threshold, and action potential amplitude remains consistent. Though we found that MSN resting membrane potential is hyperpolarized during proestrus compared with diestrus, we found concomitant hyperpolarization of the action potential

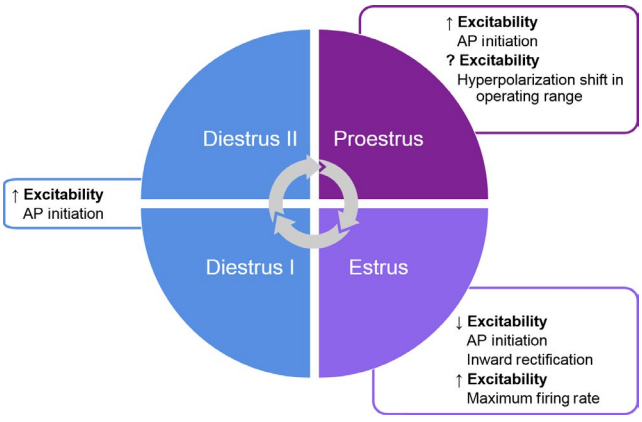

FIGURE 6 Schematic indicating changes in MSN electrical properties across estrous cycle phase. AP, action potential

threshold and increase in the action potential amplitude during proestrus, such that the operational range of the cell has simply been shifted to a more hyperpolarized state without a net change in that aspect of excitability. Consistent with this interpretation, rheobase remained relatively constant during the diestrus and proestrus phases. However, this consistency in rheobase value was not universal across the cycle. Indeed, during estrus, MSNs require significantly more excitatory current injection to initiate an action potential than during both diestrus and proestrus. Thus, regarding action potential initiation, female caudate–putamen MSNs in estrus seem less excitable than in diestrus or proestrus. These changes in MSN resting membrane potential, threshold, and rheobase implicate a number of potential targets that could be influenced by the hormones associated with the estrous cycle, including inwardly rectifying potassium currents (Jiang & North, 1991), and sustained sodium and calcium currents (Bargas, Howe, Eberwine, Cao, & Surmeier, 1994; Cepeda, Chandler, Shumate, & Levine, 1995; Chao & Alzheimer, 1995; Kita, Kita, & Kitai, 1985), slowly activating potassium currents (Nisenbaum & Wilson, 1995; Shen, Hernandez-Lopez, Tkatch, Held, & Surmeier, 2004), and signaling molecules such as acetylcholine and dopamine (Yasumoto, Tanaka, Hattori, Maeda, & Higashi, 2002).

The overall interpretation that MSNs in estrus are less excitable is further supported by the behavior of MSNs in response to hyperpolarizing current injection across the cycle. During estrus, MSNs exhibit the least amount of inward rectification compared with other phases. Conversely, during proestrus, MSN inward rectification and capacitance are increased relative to both estrus and diestrus. This suggests a potential reduction in the inwardly rectifying potassium (IRK) channel conductance during the estrus phase (Mermelstein, Song, Tkatch, Yan, & Surmeier, 1998). It follows that this decrease in inward rectification during estrus results in a greater effect of inhibitory input onto MSNs than during proestrus and diestrus and thus a decrease in excitability if the amount of inhibitory synaptic input remains unchanged. The changes in capacitance also suggest the morphological or genetic changes could be occurring in MSNs across the estrous cycle. This question remains a future avenue of research which could greatly inform our model of cyclical changes in MSN function, especially given the presence of striatal GABAergic interneurons (Fino, Vandecasteele, Perez, Saudou, & Venance, 2018), and the known estrous cycle and estradiol-induced changes in inhibitory neurotransmitter and synapse function in striatal and other brain regions such as the hippocampus (Hu, Watson, Kennedy, & Becker, 2006; Staley & Scharfman, 2005).

Thus far, these findings seem to indicate a relatively straightforward model of cyclical modulation of female MSN excitability in which MSNs in estrus are less excitable than during the other phases. This difference in excitability,

however, is specific to the properties that govern initial action potential generation and response to inhibition. A more complete picture emerges when we consider the response to strong depolarizing current injection. This is relevant to MSN physiology given that MSNs operate in multiple states including a highly depolarizing up-state (Plenz & Kitai, 1998; Wickens & Wilson, 1998). Here we detected an overall sex difference in the maximum firing rate such that female caudate–putamen MSNs reach higher peak firing rates than males. This sex difference is primarily driven by female MSNs in estrus, which demonstrated significantly higher maximum firing rates than female MSNs in proestrus. Thus, though female MSNs in estrus require more excitation to initiate an action potential than female MSNs in proestrus and diestrus, the response of the cell to strong depolarization is significantly increased. Unlike in the nucleus accumbens core (Proano et al., 2018), we detected no changes in excitatory synapse properties across the estrous cycle, which is consistent with previous work that concentrated on dendritic spine attributes (Peterson, Mermelstein, & Meisel, 2015; Staffend, Loftus, & Meisel, 2011). This does not preclude cyclical and estradiol-induced changes in excitatory synapse activity or the activity of other inputs onto MSNs, such as those associated with the dopaminergic and cholinergic systems (Calipari et al., 2017; Davis, Jacobson, Aliakbari, & Mizumori, 2005).

Taken together, these findings indicate that as female caudate–putamen MSNs progress through the estrous cycle, they become more likely to initiate an action potential during diestrus than they were during estrus. This increase in excitability persists into proestrus but is accompanied by a hyperpolarization shift in resting membrane potential and action potential threshold. Then, during estrus, the resting membrane potential and threshold shift back to a more depolarized state, but the MSN requires significantly more excitation to initiate an action potential as illustrated by increased rheobase. However, MSNs in estrus are capable of producing significantly more action potentials in response to large amount of excitatory current than during both diestrus and proestrus. The multifaceted nature of estrous cycle modulation of MSN function observed here, with phase-specific changes in action potential initiation, inward rectification properties, and action potential firing properties, suggests the presence of multiple concurrent mechanisms. This is unsurprising given that multiple hormones fluctuate over the estrous cycle which may modulate MSN physiology.

Specifically, the estrous cycle involves fluctuations in the production of the ovarian hormones progesterone and 17β-estradiol, which are capable of crossing the blood–brain barrier and acting in the brain. Decades of research have implicated estradiol in modulating striatal function (Yoest et al., 2018). Less is known regarding progesterone, although there is both recent and decade-old evidence that progesterone may also influence this brain region (Dluzen & Ramirez, 1984; Piechota et al., 2017). Focusing on estradiol, classically, estradiol acts at nuclear receptors to initiate relatively slow changes in gene transcription. However, the adult caudate–putamen does not express nuclear estrogen receptors (Almey et al., 2012), with the caveat that an exhaustive examination across all cycle phases and developmental periods has never been performed. In adult caudate–putamen, there is evidence that estradiol acts via membrane-associated estrogen receptors α, β, and GPER-1 to initiate both rapid effects on cellular function and striatal behaviors via mGluR activation, as well as triggering transcription factors such as CREB which potentially induce changes in gene expression (Almey, Milner, & Brake, 2015; Almey et al., 2012, 2016; Grove-Strawser et al., 2010; Martinez, Peterson, Meisel, & Mermelstein, 2014; Martinez et al., 2016; Meitzen et al., 2018; Mermelstein et al., 1996; Peterson et al., 2015; Song et al., 2019). Expression of these membrane-associated estrogen receptors provides a possible mechanism by which the cyclical changes in estradiol over the estrous cycle may modulate MSN excitability. Though we did not measure the level of estradiol or testosterone within the caudate–putamen for this study, there is evidence that estradiol concentration reaches significantly higher levels in the female rat caudate–putamen than in blood plasma serum and varies with the estrous cycle, peaking during proestrus (Morissette, Garcia-Segura, Belanger, & Di Paolo, 1992). The striatum also expresses the enzyme aromatase, suggesting that the region may be capable of local estradiol synthesis (Kuppers & Beyer, 1998). At least one form of striatal MSN long-term potentiation has been suggested to be dependent on local estradiol action in males (Tozzi et al., 2015), but synaptic plasticity in female MSNs across the estrous cycle remains to be explored. It is possible that the changes in female caudate–putamen MSN excitability observed here are due to a multiplexed action of local estradiol synthesis, peripheral estradiol, progesterone, or the combination of all or some of these. Just as the timing of the production and release of sex hormones over the estrous cycle triggers changes in specific neural electrical attributes, it likewise triggers changes in specific animal behaviors.

These behaviors that are modulated by the hormone changes that occur over the estrous cycle all in some way facilitate successful reproduction. During the various phases of the cycle, different suites of motor and learning behaviors occur depending on the reproductive status of the rat (Becker, 2002; Becker et al., 1987; Calhoun, 1962; Field & Pellis, 2008; Kent, Hurd, & Satinoff, 1991; Peterson, Hivick, & Lynch, 2014; Robinson, Camp, Jacknow, & Becker, 1982). For example, during proestrus, female rats exhibit increased locomotor and exploratory behavior while locating and advertising to potential mates. Then, during estrus, females predominantly stay in their nest, displaying copulatory behaviors such as lordosis. During diestrus, females are no longer sexually receptive and display less

exploratory and/or copulatory behaviors. Likewise, memory and learning shift in females from a hippocampal to striatal-based strategy depending on estrogen levels (Korol & Pisani, 2015). Modulation of striatal-dependent premotor and cognitive functions is required to facilitate the different requirements for successful reproduction across the cycle. Regarding how these behavioral changes relate to the estrous cycle-dependent modulation of MSN physiology, in the caudate–putamen, MSNs serve as the initial interpreter and modulator of inputs through the basal ganglia and causal relationships have been established between changes in MSN electrical function and behavioral endpoints (Cui et al., 2013; Ferguson, Phillips, Roth, Wess, & Neumaier, 2013; Jin, Tecuapetla, & Costa, 2014; Kravitz, Tye, & Kreitzer, 2012; Kravitz et al., 2010). Thus, estrous cycle-dependent changes in MSN physiology are likely related to changes in motor and cognitive behavior. Importantly, caudate–putamen MSNs comprise at least two major pathways, which differ in neurochemistry, dopamine receptor expression, efferent targets, gene expression, functional roles, and electrophysiological properties (Cao, Dorris, & Meitzen, 2018; Cepeda et al., 2008; Gerfen et al., 1990; Gertler, Chan, & Surmeier, 2008; Ho et al., 2018; Planert, Berger, & Silberberg, 2013; Willett et al., 2019). Future research involving MSN subtype-specificity could further illuminate the functional impact of striatal hormone action. Further, convergence of afferents into the caudate–putamen is functionally organized, yielding dorsomedial and dorsolateral sub-regions, which mediate different behaviors (Fanelli, Klein, Reese, & Robinson, 2013; Ito & Doya, 2015). Here we targeted these sub-regions equally. In order to understand the relationship between sex-specific hormone modulation of neural activity and the resultant changes in behaviors, future research should further differentiate by sub-region and determine how the other neurons involved in the circuit may be concomitantly modulated. Nevertheless, estrous cycle-dependent changes in MSN physiology could ultimately yield changes in basal ganglia circuit dynamics which in turn could induce the documented estrous cycle-dependent modulation of motor and cognitive behaviors. Given that the striatum influences these altered behaviors, and that evidence indicates that estrous cycle-induced changes in MSN excitability are present in vivo, to us it is highly likely that the properties observed to differ here contribute to alterations in behavior. At this point, however, it would be speculative to link specific changes in MSN excitability and other physiological properties with specific changes in behavior.

The estrous cycle is a phenomenon specific to adulthood, but select sex differences in MSN electrophysiology are present prior to puberty. We have previously shown that MSN excitability and excitatory synaptic input differs by sex both pre- and post-puberty in region-specific, species-specific, and estrous cycle-dependent ways (Figure 7). Female rat prepubertal caudate–putamen MSNs are more excitable than male MSNs as indicated by a hyperpolarized action potential threshold, decreased action potential afterhyperpolarization, increased initial action potential firing rate, and increased slope of the evoked action potential firing rate to injected current curve (Dorris et al., 2015). This sex difference is specific to the caudate–putamen, as MSNs in rat nucleus accumbens core and shell do not exhibit sex differences in cellular excitability during the prepubertal period (Cao, Dorris, & Meitzen, 2016; Willett et al., 2016). Similarly, no sex differences are detected in excitatory synapse properties in the caudate–putamen and nucleus accumbens shell of prepubertal rats (Dorris et al., 2015; Willett et al., 2016). Conversely, mEPSC frequency is dramatically increased in prepubertal female compared with male nucleus accumbens core MSNs and this difference is sensitive to perinatal estradiol exposure (Cao et al., 2016). The striatal regions are altered during puberty, and some sex differences do not emerge until adulthood (Andersen, Rutstein, Benzo, Hostetter, & Teicher, 1997;

Developmental effects on regional sex differences in rat MSN electrophysiology

Electrophysiological property	Developmental stage	Caudate-putamen	Nucleus accumbens core	Nucleus accumbens shell
Intrinsic excitability	Pre-puberty	F>M *Dorris et al., 2015*	F=M *Cao et al., 2016*	F=M *Willett et al., 2016*
	Post-puberty	F↺ M→ *Current Study*	F↺ M→ *Proaño et al., 2018*	?
Excitatory synapse properties	Pre-puberty	F=M *Dorris et al., 2015*	F>M *Cao et al., 2016*	F=M *Willett et al., 2016*
	Post-puberty	F=M *Current Study*	F↺ M→ *Proaño et al., 2018*	?

FIGURE 7 Developmental of regional sex and estrous cycle differences in rat MSN electrophysiological properties. symbol indicates estrous cycle-dependent sex differences were detected

Andersen, Thompson, Krenzel, & Teicher, 2002; Ghahramani et al., 2014; Kopec et al., 2018; Staffend et al., 2014). In adult female rats, Proaño and colleagues recently demonstrated estrous cycle-dependent differences in nucleus accumbens core MSN excitability and excitatory synapse properties such as mEPSC frequency and amplitude (Proano et al., 2018). Here, we detected estrous cycle-dependent differences in caudate–putamen MSN excitability without changes in excitatory synapse properties. Further, the ways in which MSN excitability is modulated in the caudate–putamen differ from the nucleus accumbens core. Given these region-specific neurodevelopmental differences in MSN physiology, future research should investigate for potential post-pubertal changes in nucleus accumbens shell MSN excitability and excitatory synapse properties. Additionally, these sex differences are species-specific as the prepubertal sex differences detected in rat caudate–putamen and nucleus accumbens core MSN are different from or absent in mice assessed during the same general developmental period (Cao et al., 2018; Willett et al., 2019). This foundational research into a single neuron type in varying regional and neuroendocrine contexts establishes the immense malleability of cellular function and the importance of considering not just animal sex, but age and hormone status when gathering and interpreting physiological data. This is illustrated by our chosen analysis paradigm, in which baseline sex differences were first compared independent of estrous cycle phase. Importantly, only one property out of the eight that differed by estrous cycle phase was also found to differ by sex when estrous cycle phase was not considered. While we are encouraged that increasing numbers of neuroscience studies are assessing females (Beery & Zucker, 2011; Shansky & Woolley, 2016; Will et al., 2017), studies that do not in some way disaggregate estrous cycle phases, whether similar to the approach employed here, a simultaneous multifactorial design, or other statistical paradigm, risk missing key variables influencing neural physiology. Nevertheless, we acknowledge that not all variables can be addressed in a single study and there are multiple factors which can influence neuron function that were not assessed in this study. Overall, this body of research demonstrates the immense heterogeneity and plasticity of fundamental cellular properties in a single neuron type, the medium spiny neuron.

ACKNOWLEDGEMENTS

We thank Drs. Jinyan Cao and Megan Serr for assistance with statistics and vaginal cytology, and the following funding sources: NIH R01MH109471 (JM), NIH P30ES025128 (Center for Human Health and the Environment), NC State University Start-up Funds (JM), and Grass Foundation Fellowship (JAW). The University of Virginia Center for Research in Reproduction Ligand Assay and Analysis Core is supported by NIH P50HD28934.

CONFLICT OF INTEREST

The authors declare no competing financial interests.

AUTHOR CONTRIBUTIONS

We confirm that this manuscript has been read and approved by all named authors and that all named authors have fulfilled the required criteria for authorship. J.A.W. contributed to the conception, execution, analysis, and interpretation; J.C. contributed to the conception and execution; A.G.J. contributed to the execution and analysis; O.P. contributed to the execution and analysis; D.M.D. contributed to the analysis; and J.M. contributed to the conception, analysis, and interpretation.

DATA ACCESSIBILITY

All data generated during this study are included in this published article.

ORCID


Jaime A. Willett https://orcid.org/0000-0003-1211-8420

REFERENCES

Almey, A., Filardo, E. J., Milner, T. A., & Brake, W. G. (2012). Estrogen receptors are found in glia and at extranuclear neuronal sites in the dorsal striatum of female rats: Evidence for cholinergic but not dopaminergic colocalization. *Endocrinology*, *153*, 5373–5383.

Almey, A., Milner, T. A., & Brake, W. G. (2015). Estrogen receptors in the central nervous system and their implication for dopamine-dependent cognition in females. *Hormones and Behavior*, *74*, 125–138.

Almey, A., Milner, T. A., & Brake, W. G. (2016). Estrogen receptor alpha and G-protein coupled estrogen receptor 1 are localised to GABAergic neurons in the dorsal striatum. *Neuroscience Letters*, *27*, 118–123.

Andersen, S. L., Rutstein, M., Benzo, J. M., Hostetter, J. C., & Teicher, M. H. (1997). Sex differences in dopamine receptor overproduction and elimination. *NeuroReport*, *8*, 1495–1498.

Andersen, S. L., Thompson, A. P., Krenzel, E., & Teicher, M. H. (2002). Pubertal changes in gonadal hormones do not underlie adolescent dopamine receptor overproduction. *Psychoneuroendocrinology*, *27*, 683–691.

Arnauld, E., Dufy, B., Pestre, M., & Vincent, J. D. (1981). Effects of estrogens on the responses of caudate neurons to microiontophoretically applied dopamine. *Neuroscience Letters*, *21*, 325–331.

Bargas, J., Howe, A., Eberwine, J., Cao, Y., & Surmeier, D. J. (1994). Cellular and molecular characterization of Ca2+ currents in acutely isolated, adult rat neostriatal neurons. *The Journal of Neuroscience*, *14*, 6667–6686.

Baufreton, J., Atherton, J. F., Surmeier, D. J., & Bevan, M. D. (2005). Enhancement of excitatory synaptic integration by GABAergic inhibition in the subthalamic nucleus. *The Journal of Neuroscience*, *25*, 8505–8517.

Bayless, D. W., & Daniel, J. M. (2015). Sex differences in myelin-associated protein levels within and density of projections between the orbital frontal cortex and dorsal striatum of adult rats: Implications for inhibitory control. *Neuroscience*, *300*, 286–296.

Beatty, W. W. (1979). Gonadal hormones and sex differences in nonreproductive behaviors in rodents: Organizational and activational influences. *Hormones and Behavior*, *12*, 112–163.

Becker, J. B. (2002). Hormonal influences on sensorimotor function. In J. Becker, S. M. Breedlove, D. Crews, & M. M. McCarthy (Eds.), *Behavioral endocrinology* (pp. 497–525). Cambridge, UK: MIT Press.

Becker, J. B., Arnold, A. P., Berkley, K. J., Blaustein, J. D., Eckel, L. A., Hampson, E., … Young, E. (2005). Strategies and methods for research on sex differences in brain and behavior. *Endocrinology*, *146*, 1650–1673.

Becker, J. B., Snyder, P. J., Miller, M. M., Westgate, S. A., & Jenuwine, M. J. (1987). The influence of estrous cycle and intrastriatal estradiol on sensorimotor performance in the female rat. *Pharmacology, Biochemistry, and Behavior*, *27*, 53–59.

Beery, A. K., & Zucker, I. (2011). Sex bias in neuroscience and biomedical research. *Neuroscience and Biobehavioral Reviews*, *35*, 565–572.

Belleau, M. L., & Warren, R. A. (2000). Postnatal development of electrophysiological properties of nucleus accumbens neurons. *Journal of Neurophysiology*, *84*, 2204–2216.

Blume, S. R., Freedberg, M., Vantrease, J. E., Chan, R., Padival, M., Record, M. J., … Rosenkranz, J. A. (2017). Sex- and estrus-dependent differences in rat basolateral amygdala. *The Journal of Neuroscience*, *37*, 10567–10586.

Butcher, R. L., Collins, W. E., & Fugo, N. W. (1974). Plasma concentration of LH, FSH, prolactin, progesterone and estradiol-17beta throughout the 4-day estrous cycle of the rat. *Endocrinology*, *94*, 1704–1708.

Calhoun, J. C. (1962). The ecology and sociology of the Norway Rat. U.S. Department of Health, Education, and Welfare, PHS NO. 1008.

Calipari, E. S., Juarez, B., Morel, C., Walker, D. M., Cahill, M. E., Ribeiro, E., … Nestler, E. J. (2017). Dopaminergic dynamics underlying sex-specific cocaine reward. *Nature Communications*, *8*, 13877.

Calizo, L. H., & Flanagan-Cato, L. M. (2000). Estrogen selectively regulates spine density within the dendritic arbor of rat ventromedial hypothalamic neurons. *The Journal of Neuroscience*, *20*, 1589–1596.

Cao, J., Dorris, D. M., & Meitzen, J. (2016). Neonatal masculinization blocks increased excitatory synaptic input in female rat nucleus accumbens core. *Endocrinology*, *157*, 3181–3196.

Cao, J., Dorris, D. M., & Meitzen, J. (2018). Electrophysiological properties of medium spiny neurons in the nucleus accumbens core of prepubertal male and female Drd1a-tdTomato line 6 BAC transgenic mice. *Journal of Neurophysiology*, *120*, 1712–1727.

Cao, J., Echelberger, R., Liu, M., Sluzas, E., McCaffrey, K., Buckley, B., & Patisaul, H. B. (2015). Soy but not bisphenol A (BPA) or the phytoestrogen genistin alters developmental weight gain and food intake in pregnant rats and their offspring. *Reproductive Toxicology*, *58*, 282–294.

Castrioto, A., Hulliger, S., Poon, Y. Y., Lang, A. E., & Moro, E. (2010). A survey on the impact of the menstrual cycle on movement disorders severity. *Canadian Journal of Neurological Sciences/Journal Canadien des Sciences Neurologiques*, *37*, 478–481.

Cepeda, C., Andre, V. M., Yamazaki, I., Wu, N., Kleiman-Weiner, M., & Levine, M. S. (2008). Differential electrophysiological properties of dopamine D1 and D2 receptor-containing striatal medium-sized spiny neurons. *The European Journal of Neuroscience*, *27*, 671–682.

Cepeda, C., Chandler, S. H., Shumate, L. W., & Levine, M. S. (1995). Persistent Na+ conductance in medium-sized neostriatal neurons: Characterization using infrared videomicroscopy and whole cell patch-clamp recordings. *Journal of Neurophysiology*, *74*, 1343–1348.

Chao, T. I., & Alzheimer, C. (1995). Do neurons from rat neostriatum express both a TTX-sensitive and a TTX-insensitive slow Na+ current? *Journal of Neurophysiology*, *74*, 934–941.

Cooke, B. M., & Woolley, C. S. (2005). Gonadal hormone modulation of dendrites in the mammalian CNS. *Journal of Neurobiology*, *64*, 34–46.

Cui, G., Jun, S. B., Jin, X., Pham, M. D., Vogel, S. S., Lovinger, D. M., & Costa, R. M. (2013). Concurrent activation of striatal direct and indirect pathways during action initiation. *Nature*, *494*, 238–242.

Davis, D. M., Jacobson, T. K., Aliakbari, S., & Mizumori, S. J. (2005). Differential effects of estrogen on hippocampal- and striatal-dependent learning. *Neurobiology of Learning and Memory*, *84*, 132–137.

Di Paolo, T. (1994). Modulation of brain dopamine transmission by sex steroids. *Reviews in the Neurosciences*, *5*, 27–41.

Dluzen, D. E., & Ramirez, V. D. (1984). Bimodal effect of progesterone on in vitro dopamine function of the rat corpus striatum. *Neuroendocrinology*, *39*, 149–155.

Dorris, D. M., Cao, J., Willett, J. A., Hauser, C. A., & Meitzen, J. (2015). Intrinsic excitability varies by sex in pre-pubertal striatal medium spiny neurons. *Journal of Neurophysiology*, *113*, 720–729.

Dorris, D. M., Hauser, C. A., Minnehan, C. E., & Meitzen, J. (2014). An aerator for brain slice experiments in individual cell culture plate wells. *Journal of Neuroscience Methods*, *238*, 1–10.

Fanelli, R. R., Klein, J. T., Reese, R. M., & Robinson, D. L. (2013). Dorsomedial and dorsolateral striatum exhibit distinct phasic neuronal activity during alcohol self-administration in rats. *The European Journal of Neuroscience*, *38*, 2637–2648.

Farries, M. A., Meitzen, J., & Perkel, D. J. (2005). Electrophysiological properties of neurons in the basal ganglia of the domestic chick: Conservation and divergence in the evolution of the avian basal ganglia. *Journal of Neurophysiology*, *94*, 454–467.

Farries, M. A., & Perkel, D. J. (2000). Electrophysiological properties of avian basal ganglia neurons recorded in vitro. *Journal of Neurophysiology*, *84*, 2502–2513.

Farries, M. A., & Perkel, D. J. (2002). A telencephalic nucleus essential for song learning contains neurons with physiological characteristics of both striatum and globus pallidus. *The Journal of Neuroscience*, *22*, 3776–3787.

Ferguson, S. M., Eskenazi, D., Ishikawa, M., Wanat, M. J., Phillips, P. E., Dong, Y., … Neumaier, J. F. (2011). Transient neuronal inhibition reveals opposing roles of indirect and direct pathways in sensitization. *Nature Neuroscience*, *14*, 22–24.

Ferguson, S. M., Phillips, P. E., Roth, B. L., Wess, J., & Neumaier, J. F. (2013). Direct-pathway striatal neurons regulate the retention of decision-making strategies. *The Journal of Neuroscience*, *33*, 11668–11676.

Field, E. F., & Pellis, S. M. (2008). The brain as the engine of sex differences in the organization of movement in rats. *Archives of Sexual Behavior*, *37*, 30–42.

Fino, E., Vandecasteele, M., Perez, S., Saudou, F., & Venance, L. (2018). Region-specific and state-dependent action of striatal GABAergic interneurons. *Nature Communications*, *9*, 3339.

Forlano, P. M., & Woolley, C. S. (2010). Quantitative analysis of pre- and postsynaptic sex differences in the nucleus accumbens. *The Journal of Comparative Neurology*, *518*, 1330–1348.

Gerfen, C. R., Engber, T. M., Mahan, L. C., Susel, Z., Chase, T. N., Monsma, F. J. Jr, & Sibley, D. R. (1990). D1 and D2 dopamine receptor-regulated gene expression of striatonigral and striatopallidal neurons. *Science*, *250*, 1429–1432.

Gertler, T. S., Chan, C. S., & Surmeier, D. J. (2008). Dichotomous anatomical properties of adult striatal medium spiny neurons. *The Journal of Neuroscience*, *28*, 10814–10824.

Ghahramani, N. M., Ngun, T. C., Chen, P. Y., Tian, Y., Krishnan, S., Muir, S., … Vilain, E. (2014). The effects of perinatal testosterone exposure on the DNA methylome of the mouse brain are late-emerging. *Biology of Sex Differences*, *5*, 8.

Gillies, G. E., & McArthur, S. (2010). Estrogen actions in the brain and the basis for differential action in men and women: A case for sex-specific medicines. *Pharmacological Reviews*, *62*, 155–198.

Grillner, S., Hellgren, J., Menard, A., Saitoh, K., & Wikstrom, M. A. (2005). Mechanisms for selection of basic motor programs–roles for the striatum and pallidum. *Trends in Neurosciences*, *28*, 364–370.

Grove-Strawser, D., Boulware, M. I., & Mermelstein, P. G. (2010). Membrane estrogen receptors activate the metabotropic glutamate receptors mGluR5 and mGluR3 to bidirectionally regulate CREB phosphorylation in female rat striatal neurons. *Neuroscience*, *170*, 1045–1055.

Hampson, E. (1990). Estrogen-related variations in human spatial and articulatory-motor skills. *Psychoneuroendocrinology*, *15*, 97–111.

Hampson, E., & Kimura, D. (1988). Reciprocal effects of hormonal fluctuations on human motor and perceptual-spatial skills. *Behavioral Neuroscience*, *102*, 456–459.

Hao, J., Rapp, P. R., Leffler, A. E., Leffler, S. R., Janssen, W. G., Lou, W., … Morrison, J. H. (2006). Estrogen alters spine number and morphology in prefrontal cortex of aged female rhesus monkeys. *The Journal of Neuroscience*, *26*, 2571–2578.

Hicks, K. D., Sullivan, A. W., Cao, J., Sluzas, E., Rebuli, M., & Patisaul, H. B. (2016). Interaction of bisphenol A (BPA) and soy phytoestrogens on sexually dimorphic sociosexual behaviors in male and female rats. *Hormones and Behavior*, *84*, 121–126.

Ho, H., Both, M., Siniard, A., Sharma, S., Notwell, J. H., Wallace, M., … Portmann, T. (2018). A guide to single-cell transcriptomics in adult rodent brain: The medium spiny neuron transcriptome revisited. *Frontiers in Cellular Neuroscience*, *12*, 159.

Hu, M., Watson, C. J., Kennedy, R. T., & Becker, J. B. (2006). Estradiol attenuates the K+-induced increase in extracellular GABA in rat striatum. *Synapse (New York, N. Y.)*, *59*, 122–124.

Hubscher, C. H., Brooks, D. L., & Johnson, J. R. (2005). A quantitative method for assessing stages of the rat estrous cycle. *Biotechnic & Histochemistry*, *80*, 79–87.

Ito, M., & Doya, K. (2015). Distinct neural representation in the dorsolateral, dorsomedial, and ventral parts of the striatum during fixed- and free-choice tasks. *The Journal of Neuroscience*, *35*, 3499–3514.

Jennings, P. J., Janowsky, J. S., & Orwoll, E. (1998). Estrogen and sequential movement. *Behavioral Neuroscience*, *112*, 154–159.

Jiang, Z. G., & North, R. A. (1991). Membrane properties and synaptic responses of rat striatal neurones in vitro. *The Journal of Physiology*, *443*, 533–553.

Jin, X., Tecuapetla, F., & Costa, R. M. (2014). Basal ganglia subcircuits distinctively encode the parsing and concatenation of action sequences. *Nature Neuroscience*, *17*, 423–430.

Juraska, J. M., Sisk, C. L., & DonCarlos, L. L. (2013). Sexual differentiation of the adolescent rodent brain: Hormonal influences and developmental mechanisms. *Hormones and Behavior*, *64*, 203–210.

Kawaguchi, Y., Wilson, C. J., & Emson, P. C. (1989). Intracellular recording of identified neostriatal patch and matrix spiny cells in a slice preparation preserving cortical inputs. *Journal of Neurophysiology*, *62*, 1052–1068.

Kent, S., Hurd, M., & Satinoff, E. (1991). Interactions between body temperature and wheel running over the estrous cycle in rats. *Physiology & Behavior*, *49*, 1079–1084.

Kita, H., Kita, T., & Kitai, S. T. (1985). Regenerative potentials in rat neostriatal neurons in an in vitro slice preparation. *Experimental Brain Research*, *60*, 63–70.

Kopec, A. M., Smith, C. J., Ayre, N. R., Sweat, S. C., & Bilbo, S. D. (2018). Microglial dopamine receptor elimination defines sex-specific nucleus accumbens development and social behavior in adolescent rats. *Nature Communications*, *9*, 3769.

Korol, D. L., & Pisani, S. L. (2015). Estrogens and cognition: Friends or foes?: An evaluation of the opposing effects of estrogens on learning and memory. *Hormones and Behavior*, *74*, 105–115.

Kravitz, A. V., Freeze, B. S., Parker, P. R., Kay, K., Thwin, M. T., Deisseroth, K., & Kreitzer, A. C. (2010). Regulation of parkinsonian motor behaviours by optogenetic control of basal ganglia circuitry. *Nature*, *466*, 622–626.

Kravitz, A. V., Tye, L. D., & Kreitzer, A. C. (2012). Distinct roles for direct and indirect pathway striatal neurons in reinforcement. *Nature Neuroscience*, *15*, 816–818.

Kreitzer, A. C., & Malenka, R. C. (2008). Striatal plasticity and basal ganglia circuit function. *Neuron*, *60*, 543–554.

Kuppers, E., & Beyer, C. (1998). Expression of aromatase in the embryonic and postnatal mouse striatum. *Brain Research. Molecular Brain Research*, *63*, 184–188.

Martinez, L. A., Gross, K. S., Himmler, B. T., Emmitt, N. L., Peterson, B. M., Zlebnik, N. E., … Mermelstein, P. G. (2016). Estradiol facilitation of cocaine self-administration in female rats requires activation of mGluR5. *eNeuro*, *3*, ENEURO.0140-0116.2016.

Martinez, L. A., Peterson, B. M., Meisel, R. L., & Mermelstein, P. G. (2014). Estradiol facilitation of cocaine-induced locomotor sensitization in female rats requires activation of mGluR5. *Behavioural Brain Research*, *271*, 39–42.

Meitzen, J., Meisel, R. L., & Mermelstein, P. G. (2018). Sex differences and the effects of estradiol on striatal function. *Current Opinion in Behavioral Sciences*, *23*, 42–48.

Meitzen, J., Pflepsen, K. R., Stern, C. M., Meisel, R. L., & Mermelstein, P. G. (2011). Measurements of neuron soma size and density in rat dorsal striatum, nucleus accumbens core and nucleus accumbens shell: Differences between striatal region and brain hemisphere, but not sex. *Neuroscience Letters*, *487*, 177–181.

Meitzen, J., Weaver, A. L., Brenowitz, E. A., & Perkel, D. J. (2009). Plastic and stable electrophysiological properties of adult avian forebrain song-control neurons across changing breeding conditions. *The Journal of Neuroscience*, *29*, 6558–6567.

Mermelstein, P. G., Becker, J. B., & Surmeier, D. J. (1996). Estradiol reduces calcium currents in rat neostriatal neurons via a membrane receptor. *The Journal of Neuroscience*, *16*, 595–604.

Mermelstein, P. G., Song, W. J., Tkatch, T., Yan, Z., & Surmeier, D. J. (1998). Inwardly rectifying potassium (IRK) currents are correlated with IRK subunit expression in rat nucleus accumbens medium spiny neurons. *The Journal of Neuroscience*, *18*, 6650–6661.

Micevych, P. E., & Meisel, R. L. (2017). Integrating neural circuits controlling female sexual behavior. *Frontiers in Systems Neuroscience*, *11*, 42.

Morissette, M., Garcia-Segura, L. M., Belanger, A., & Di Paolo, T. (1992). Changes of rat striatal neuronal membrane morphology and steroid content during the estrous cycle. *Neuroscience*, *49*, 893–902.

Mu, P., Moyer, J. T., Ishikawa, M., Zhang, Y., Panksepp, J., Sorg, B. A., … Dong, Y. (2010). Exposure to cocaine dynamically regulates the intrinsic membrane excitability of nucleus accumbens neurons. *The Journal of Neuroscience*, *30*, 3689–3699.

Nisenbaum, E. S., Xu, Z. C., & Wilson, C. J. (1994). Contribution of a slowly inactivating potassium current to the transition to firing of neostriatal spiny projection neurons. *J Neurophysiol*, *71*(3), 1174–1189. https://doi.org/10.1152/jn.1994.71.3.1174

Nisenbaum, E. S., & Wilson, C. J. (1995). Potassium currents responsible for inward and outward rectification in rat neostriatal spiny projection neurons. *The Journal of Neuroscience*, *15*, 4449–4463.

O'Donnell, P., & Grace, A. A. (1993). Physiological and morphological properties of accumbens core and shell neurons recorded in vitro. *Synapse (New York, N. Y.)*, *13*, 135–160.

Okamoto, K., Hirata, H., Takeshita, S., & Bereiter, D. A. (2003). Response properties of TMJ units in superficial laminae at the spinomedullary junction of female rats vary over the estrous cycle. *Journal of Neurophysiology*, *89*, 1467–1477.

Palmiter, R. D. (2008). Dopamine signaling in the dorsal striatum is essential for motivated behaviors: Lessons from dopamine-deficient mice. *Annals of the New York Academy of Sciences*, *1129*, 35–46.

Peterson, A. B., Hivick, D. P., & Lynch, W. J. (2014). Dose-dependent effectiveness of wheel running to attenuate cocaine-seeking: Impact of sex and estrous cycle in rats. *Psychopharmacology (Berl)*, *231*, 2661–2670.

Peterson, B. M., Mermelstein, P. G., & Meisel, R. L. (2015). Estradiol mediates dendritic spine plasticity in the nucleus accumbens core through activation of mGluR5. *Brain Structure and Function*, *220*, 2415–2422.

Piechota, M., Korostynski, M., Golda, S., Ficek, J., Jantas, D., Barbara, Z., & Przewlocki, R. (2017). Transcriptional signatures of steroid hormones in the striatal neurons and astrocytes. *BMC Neuroscience*, *18*, 37.

Planert, H., Berger, T. K., & Silberberg, G. (2013). Membrane properties of striatal direct and indirect pathway neurons in mouse and rat slices and their modulation by dopamine. *PLoS ONE*, *8*, e57054.

Plenz, D., & Kitai, S. T. (1998). Up and down states in striatal medium spiny neurons simultaneously recorded with spontaneous activity in fast-spiking interneurons studied in cortex-striatum-substantia nigra organotypic cultures. *The Journal of Neuroscience*, *18*, 266–283.

Proano, S., Morris, H. J., Kunz, L. M., Dorris, D. M., & Meitzen, J. (2018). Estrous cycle-induced sex differences in medium spiny neuron excitatory synaptic transmission and intrinsic excitability in adult rat nucleus accumbens core. *Journal of Neurophysiology*, *120*, 1356–1373.

Quinn, N. P., & Marsden, C. D. (1986). Menstrual-related fluctuations in Parkinson's disease. *Movement Disorders*, *1*, 85–87.

Robinson, T. E., Camp, D. M., Jacknow, D. S., & Becker, J. B. (1982). Sex differences and estrous cycle dependent variation in rotational behavior elicited by electrical stimulation of the mesostriatal dopamine system. *Behavioural Brain Research*, *6*, 273–287.

Schultz, K. N., von Esenwein, S. A., Hu, M., Bennett, A. L., Kennedy, R. T., Musatov, S., … Becker, J. B. (2009). Viral vector-mediated overexpression of estrogen receptor-alpha in striatum enhances the estradiol-induced motor activity in female rats and estradiol-modulated GABA release. *The Journal of Neuroscience*, *29*, 1897–1903.

Shansky, R. M., & Woolley, C. S. (2016). Considering sex as a biological variable will be valuable for neuroscience research. *The Journal of Neuroscience*, *36*, 11817–11822.

Shen, W., Hernandez-Lopez, S., Tkatch, T., Held, J. E., & Surmeier, D. J. (2004). Kv1.2-containing K+ channels regulate subthreshold excitability of striatal medium spiny neurons. *Journal of Neurophysiology*, *91*, 1337–1349.

Simic, N., Tokic, A., & Pericic, M. (2010). Performance of fine motor and spatial tasks during the menstrual cycle. *Arhiv za Higijenu Rada i Toksikologiju*, *61*, 407–414.

Smith, S. S. (1994). Female sex steroid hormones: From receptors to networks to performance–actions on the sensorimotor system. *Progress in Neurobiology*, *44*, 55–86.

Song, Z., Yang, H., Peckham, E. M., & Becker, J. B. (2019). Estradiol-induced potentiation of dopamine release in dorsal striatum following amphetamine administration requires estradiol receptors and mGlu5. *eNeuro*, *6*, pii: ENEURO.0446-0418.2019.

Staffend, N. A., Loftus, C. M., & Meisel, R. L. (2011). Estradiol reduces dendritic spine density in the ventral striatum of female Syrian hamsters. *Brain Structure and Function*, *215*, 187–194.

Staffend, N. A., Mohr, M. A., Doncarlos, L. L., & Sisk, C. L. (2014). A decrease in the addition of new cells in the nucleus accumbens and prefrontal cortex between puberty and adulthood in male rats. *Developmental Neurobiology*, *74*, 633–642.

Staley, K., & Scharfman, H. (2005). A woman's prerogative. *Nature Neuroscience*, *8*, 697–699.

Tan, C. L., Plotkin, J. L., Veno, M. T., von Schimmelmann, M., Feinberg, P., Mann, S., … Schaefer, A. (2013). MicroRNA-128 governs neuronal excitability and motor behavior in mice. *Science*, *342*, 1254–1258.

Tansey, E. M., Arbuthnott, G. W., Fink, G., & Whale, D. (1983). Oestradiol-17 beta increases the firing rate of antidromically identified neurones of the rat neostriatum. *Neuroendocrinology*, *37*, 106–110.

Tozzi, A., de Iure, A., Tantucci, M., Durante, V., Quiroga-Varela, A., Giampa, C., … Calabresi, P. (2015). Endogenous 17beta-estradiol is required for activity-dependent long-term potentiation in the striatum: Interaction with the dopaminergic system. *Frontiers in Cellular Neuroscience*, *9*. https://doi.org/10.3389/fncel.2015.00192

Westwood, F. R. (2008). The female rat reproductive cycle: A practical histological guide to staging. *Toxicologic Pathology*, *36*, 375–384.

Wickens, J. R., & Wilson, C. J. (1998). Regulation of action-potential firing in spiny neurons of the rat neostriatum in vivo. *Journal of Neurophysiology*, *79*, 2358–2364.

Wierman, M. E., Auchus, R. J., Haisenleder, D. J., Hall, J. E., Handelsman, D., Hankinson, S., … Stanczyk, F. Z. (2014). Editorial: The new instructions to authors for the reporting of steroid hormone measurements. *Endocrinology*, *155*, 4603.

Will, T. R., Proano, S. B., Thomas, A. M., Kunz, L. M., Thompson, K. C., Ginnari, L. A., … Meitzen, J. (2017). Problems and progress regarding sex bias and omission in neuroscience research. *eNeuro*, *4*.

Willett, J. A., Cao, J., Dorris, D. M., Johnson, A. G., Ginnari, L. A., & Meitzen, J. (2019). Electrophysiological properties of male and female medium spiny neuron subtypes in the caudate putamen of Drd1a-tdTomato line 6 BAC transgenic mice. *eNeuro*, *6* [Epub ahead of Print].

Willett, J. A., Johnson, A. G., Vogel, A. R., Patisaul, H. B., McGraw, L. A., & Meitzen, J. (2018). Nucleus accumbens core medium spiny neuron electrophysiological properties and partner preference behavior in the adult male prairie vole, Microtus ochrogaster. *Journal of Neurophysiology*, *119*, 1576–1588.

Willett, J. A., Will, T. R., Hauser, C. A., Dorris, D. M., Cao, J., & Meitzen, J. (2016). No evidence for sex differences in the electrophysiological properties and excitatory synaptic input onto nucleus accumbens shell medium spiny neurons. *eNeuro*, *3*, pii: ENEURO.0147-0115.2016.

Wissman, A. M., May, R. M., & Woolley, C. S. (2012). Ultrastructural analysis of sex differences in nucleus accumbens synaptic connectivity. *Brain Structure and Function*, *217*, 181–190.

Wissman, A. M., McCollum, A. F., Huang, G. Z., Nikrodhanond, A. A., & Woolley, C. S. (2011). Sex differences and effects of cocaine on excitatory synapses in the nucleus accumbens. *Neuropharmacology*, *61*, 217–227.

Wong, J. E., Cao, J., Dorris, D. M., & Meitzen, J. (2016). Genetic sex and the volumes of the caudate-putamen, nucleus accumbens core and shell: Original data and a review. *Brain Structure and Function*, *221*, 4257–4267.

Woolley, C. S. (1998). Estrogen-mediated structural and functional synaptic plasticity in the female rat hippocampus. *Hormones and Behavior*, *34*, 140–148.

Woolley, C. S., & McEwen, B. S. (1993). Roles of estradiol and progesterone in regulation of hippocampal dendritic spine density during the estrous cycle in the rat. *The Journal of Comparative Neurology*, *336*, 293–306.

Yasumoto, S., Tanaka, E., Hattori, G., Maeda, H., & Higashi, H. (2002). Direct and indirect actions of dopamine on the membrane potential in medium spiny neurons of the mouse neostriatum. *Journal of Neurophysiology*, *87*, 1234–1243.

Yoest, K. E., Quigley, J. A., & Becker, J. B. (2018). Rapid effects of ovarian hormones in dorsal striatum and nucleus accumbens. *Hormones and Behavior*, *104*, 119–129.

Zoghi, M., Vaseghi, B., Bastani, A., Jaberzadeh, S., & Galea, M. P. (2015). The effects of sex hormonal fluctuations during menstrual cycle on cortical excitability and manual dexterity (a pilot study). *PLoS ONE*, *10*, e0136081.

How to cite this article: Willett JA, Cao J, Johnson A, Patel OH, Dorris DM, Meitzen J. The estrous cycle modulates rat caudate–putamen medium spiny neuron physiology. *Eur J Neurosci*. 2020;52:2737–2755. https://doi.org/10.1111/ejn.14506